Accelerated Publications

A Low-Redox Potential Heme in the Dinuclear Center of Bacterial Nitric Oxide Reductase: Implications for the Evolution of Energy-Conserving Heme−Copper Oxidases†

Karin L. C. Grönberg,‡,§ M. Dolores Roldán,§,|| Louise Prior,‡ Gareth Butland,|| Myles R. Cheesman,‡ David J. Richardson,|| Stephen Spiro,|| Andrew J. Thomson,‡ and Nicholas J. Watmough*,||

Centre for Metalloprotein Spectroscopy and Biology, School of Biological Sciences and School of Chemical Sciences, University of East Anglia, Norfolk NR4 7TJ, United Kingdom

Received July 16, 1999; Revised Manuscript Received August 30, 1999

ABSTRACT: Bacterial nitric oxide reductase (NOR) catalyzes the two-electron reduction of nitric oxide to nitrous oxide. It is a highly diverged member of the superfamily of heme−copper oxidases. The main feature by which NOR is distinguished from the heme−copper oxidases is the elemental composition of the active site, a dinuclear center comprised of heme b_3 and non-heme iron (Fe_B). The visible region electronic absorption spectrum of *reduced* NOR exhibits a maximum at 551 nm with a distinct shoulder at 560 nm; these are attributed to Fe(II) heme *c* (E_m = 310 mV) and Fe(II) heme *b* (E_m = 345 mV), respectively. The electronic absorption spectrum of *oxidized* NOR exhibits a characteristic shoulder around 595 nm that exhibits complex behavior in equilibrium redox titrations. The first phase of reduction is characterized by an apparent shift of the shoulder to 604 nm and a decrease in intensity. This is due to reduction of Fe_B (E_m = 320 mV), while the subsequent bleaching of the 604 nm band represents reduction of heme b_3 (E_m = 60 mV). This separation of redox potentials (>200 mV) allows the enzyme to be poised in the three-electron reduced state for detailed spectroscopic examination of the Fe(III) heme b_3 center. The low midpoint potential of heme b_3 represents a thermodynamic barrier to the complete (two-electron) reduction of the dinuclear center. This may avoid formation of a stable Fe(II) heme b_3−NO species during turnover, which may be an inhibited state of the enzyme. It would also appear that the evolution of significant oxygen reducing activity by heme−copper oxidases was not simply a matter of the substitution of copper for non-heme iron in the dinuclear center. Changes in the protein environment that modulate the midpoint redox potential of heme b_3 to facilitate both complete reduction of the dinuclear center (a prerequisite for oxygen binding) and rapid heme−heme electron transfer were also necessary.

Nitric oxide reductase (NOR)[1] is an enzyme of bacterial denitrification which catalyzes the two-electron reduction of NO to N_2O (*1*, *2*). It is the subject of much current interest because of its close structural relationship to the proton motive heme−copper oxidases (*3*). This relationship, originally uncovered by primary sequence analysis (*4*, *5*), is reflected in similarities in organization and ligation of the hemes found in the catalytic subunits of NOR and heme−copper oxidases (*6*). The essential difference between the two classes of enzymes lies in the organization of the active site. In oxidized heme−copper oxidases, this comprises a heme lying within 5 Å of a copper ion (Cu_B) (*7*, *8*) to form a magnetically interacting dinuclear center (*9*). Elemental analyses of NOR purified from a number of bacterial sources have failed to reveal the presence of any copper. However, these analyses consistently indicate that there are 4 equiv of iron per mole of enzyme, rather than the 3 equiv that might be expected on the basis of heme content alone (*10*, *11*). Hence, it has been suggested that the dinuclear center of NOR consists of heme coupled to non-heme iron (Fe_B) rather than copper, and there is now spectroscopic evidence to support this (*6*, *11*, *12*).

NOR from *Paracoccus denitrificans*, a Gram-negative soil bacterium, is usually isolated as a heterodimer NorBC (*11*−*13*). The catalytic subunit, NorB, is a 53 kDa (apparent molecular mass of 40−45 kDa as determined by SDS−PAGE) polypeptide, comprising 12 transmembrane helices

† Supported by grants from the Commission of the European Communities (BIO4-CT98-0507), UK BBSRC (83/C10160 and BO30321), and the Wellcome Trust (054798/Z/98/Z).

* To whom correspondence should be addressed. Telephone: +44 (1603) 592179. Fax: +44 (1603) 592250. E-mail: n.watmough@uea.ac.uk.

‡ School of Chemical Sciences.

§ These authors contributed equally to this work.

|| School of Biological Sciences.

[1] Abbreviations: C*c*O, cytochrome *c* oxidase; CT band, charge-transfer band; DM, dodecyl β-D-maltoside; E_h, actual redox potential at a specified pH; E_m, midpoint redox potential at a specified pH; EPR, electron paramagnetic resonance; pH*, apparent pH at room temperature of a buffer made in D_2O; RT-MCD, room-temperature magnetic circular dichroism.

10.1021/bi9916426 CCC: $18.00
Published on Web 09/30/1999

(*5*), that contains both the low-spin bis-histidine coordinated heme *b* and the heme b_3-Fe_B dinuclear center (*11*, *12*).[2] NorC is predicted to have a single transmembrane helix at the N-terminus that anchors the periplasmic C-terminus to the cytoplasmic membrane. A single Cys-Xaa-Xaa-Cys-His *c*-type heme binding motif has been identified in this domain (*14*). This observation is consistent with biochemical analysis that shows that NorC is a membrane-anchored 17 kDa monoheme *c*-type cytochrome (*13*).

The mechanism by which NOR reduces NO to N_2O has not yet been elucidated. As a first step in investigating this mechanism, we have used mediated redox potentiometry to measure the midpoint redox potentials of each of the metal centers in NOR. We show that heme b_3 has an unexpectedly low midpoint redox potential, which would make full reduction of the dinuclear center thermodynamically unfavorable. This may represent the mechanism by which bacterial NOR avoids the formation of a potentially dead-end Fe(II)−heme b_3−NO species during turnover.

MATERIALS AND METHODS

Cell Growth and Enzyme Purification. The source of the NOR used in this study was *P. denitrificans* strain 93.11 (Δ*cta*DI, Δ*cta*DII *qox*B::*kan*^{R}) (*15*) grown in batch culture in minimal medium under anaerobic denitrifying conditions. The two-subunit form of the enzyme was purified according to the method of Hendriks et al. (*11*) with minor modifications. The purified enzyme was >95% pure as judged by SDS−PAGE, with an A_{280}/A_{410} ratio of 1.1 and a specific activity of 7 μmol of NO mg^{-1} min^{-1} as determined polarographically (*16*).

Spectroscopy. Electronic absorbance spectra were recorded on either a Hitachi U3000 or an Aminco DW2000 spectrophotometer. Spectra were exported as ASCII files and replotted in Origin v5.0 (Microcal). EPR spectra were recorded on an X-band ER-200D spectrometer (Bruker Spectrospin) interfaced with an ESP 1600 computer and fitted with a liquid helium flow cryostat (ESR-9, Oxford Instruments). MCD spectra were recorded on circular dichrographs (Jasco models J-500D and J-730). An Oxford Instruments superconducting solenoid with a 25 mm room-temperature bore was used to generate magnetic fields of up to 6 T. MCD spectral intensities depend linearly on the magnetic field at room temperature and are expressed per unit magnetic field as $\Delta\epsilon/H$ (M^{-1} cm^{-1} T^{-1}). The concentration of NOR was calculated using an ϵ_{411} of 3.11×10^5 M^{-1} cm^{-1} (*6*).

Redox Potentiometry. Mediated redox titrations of NOR were carried out at 20 °C in buffer containing 20 mM Tris-HCl, 0.02% DM, 0.34 M NaCl, and 0.5 mM EDTA (pH* 7.6) essentially as described by Dutton (*17*). Dithionite was used as the reductant and potassium ferricyanide as the oxidant. The redox mediators, each at a final concentration of 20 μM, were phenazine methosulfate, phenazine ethosulfate, diaminodurene, juglone, 5-anthraquinone 2-sulfonate, 6-anthraquinone 2,6-disulfonate, and benzyl viologen. Quinhydrone was used as a redox standard (E_m = 295 mV). All potentials quoted are with respect to the standard hydrogen electrode.

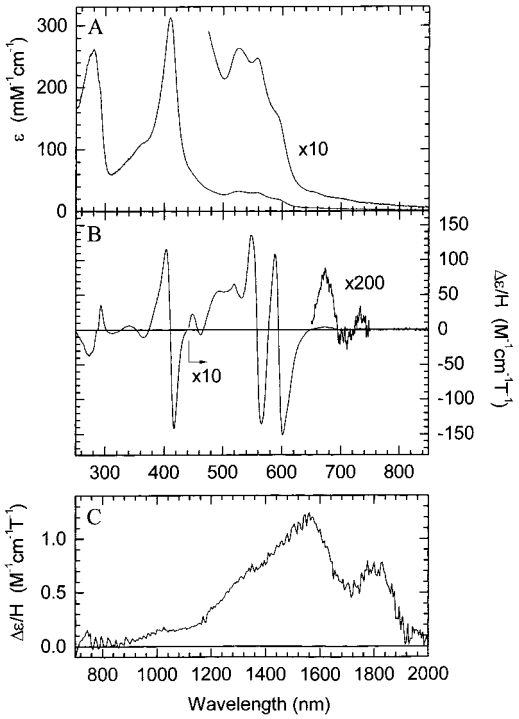

FIGURE 1: Electronic absorption, and MCD spectra of oxidized *P. denitrificans* NOR. (A) The UV−visible region electronic absorption spectrum recorded at room temperature. (B) The UV−visible region RT-MCD spectrum. (C) The near-infrared RT-MCD spectrum. In each case, the sample was 175 μM oxidized NOR in 20 mM Tris-HCl and 0.02% (w/v) DM (pH* 7.6).

Preparation of Three-Electron-Reduced NOR for MCD Spectroscopy. All manipulations were carried out in an anaerobic (<1 ppm O_2) chamber (Belle Technology, Portesham, U.K.). A 180 μL sample of 35 μM NOR in 20 mM Tris-HCl, 0.02% DM, 0.34 M NaCl, and 0.5 mM EDTA (pH* 7.6) supplemented with potassium ferricyanide and the cocktail of redox mediators described above was placed into an Al_2O_3-polished carbon cell. A reference electrode (Ag/AgCl) and a platinum foil counter electrode were introduced into the protein solution. Reduction of NOR was monitored using an Autolab electrochemical analyzer (EcoChemie, Utrecht, The Netherlands) controlled by GPES software. The redox potential was maintained at 150 mV (with respect to the standard hydrogen electrode) at 15 °C for 90 min, before the sample was transferred to an anaerobic cell for MCD spectroscopy.

RESULTS

Electronic Absorption and MCD Spectra of Oxidized NOR. The UV−visible region electronic absorption spectrum of the oxidized enzyme (Figure 1A) exhibits a Soret band at 411 nm, two broad but resolved peaks in the α,β region at

[2] The metal centers of NOR. To aid in the comparison with the heme−copper oxidases, we have adopted the following notation for the metal centers in NorB which is structurally related to C*c*O subunit I. Heme *b* is the low-spin bis-histidine coordinated heme in NorB that is a homologue of heme *a* in C*c*O. Heme b_3 is high-spin in NorB and equivalent to heme a_3 in C*c*O and heme o_3 of *E. coli* cytochrome bo_3 quinol oxidase. In C*c*O and quinol oxidases, this heme is magnetically coupled to a copper ion (Cu_B) to form a dinuclear center which is the site of oxygen binding and reduction. Fe_B is a non-heme iron in NorB, which is probably ligated by three conserved histidine residues, which serve as ligands to Cu_B in C*c*O. A fourth metal center, heme *c*, is a covalently bound low-spin heme in NorC with histidine and methionine axial ligands. This site has no structural counterpart in C*c*O, but is functionally equivalent to Cu_A in that it serves as a site of electron input for the respiratory complex.

530 and 560 nm, a distinct shoulder near 595 nm, and weak features between 640 and 740 nm. Porphyrin-based $\pi-\pi^*$ transitions from all three ferric hemes will contribute both to the Soret and to the α,β regions. At wavelengths longer than ~580 nm, additional charge-transfer (CT) transitions can occur in specific cases. A shoulder to the red of the α,β absorption envelope is typical of the porphyrin-to-ferric CT transition characteristic of high-spin ferric heme. Such a feature, traditionally termed the "630-band", is usually observed at significantly longer wavelengths, for example, in metmyoglobins where the ferric heme has histidine and/or water ligation. However, in hemes with proximal histidine coordination, e.g., heme b_3, this band shifts to the blue in the presence of anionic distal ligands such as fluoride, hydroxide, and tyrosinate. Weak absorption features between 640 and 740 nm (often termed the "695-intensity") are assigned as the S → Fe(III) CT intensity associated with the methionine ligand of ferric heme *c* in NorC.

The room-temperature MCD spectrum (Figure 1B) provides important additional information concerning the electronic properties of the hemes in NOR. The Soret band will be dominated by low-spin ferric hemes; high-spin contributions are at least 1 order of magnitude less intense. Here the observed peak-to-trough intensity of ~250 M^{-1} cm^{-1} T^{-1} points to only two of the three ferric hemes being low-spin. Absorption bands attributed to ferric heme *c* with methionine as an axial ligand in the 640−740 nm region appear in the MCD as a weak derivative feature similar to that observed for *Pseudomonas stutzeri* NOR (*6*).

The MCD of *P. denitrificans* NOR differs from the *Ps. stutzeri* enzyme in the α,β region in that *two* sharp derivative features are observed centered at 559 and 595 nm (Figure 1B) rather than a single derivative at 559 nm (*6*). The 559 nm derivative of the *P. denitrificans* NOR MCD spectrum has an intensity expected for *one* low-spin ferric heme, whereas for the *Ps. stutzeri* enzyme, the derivative at the same wavelength, which was assigned to heme *b and* heme *c*, exhibits almost twice the intensity (*6*). In Figure 1B, the intensity of the second derivative feature at 595 nm is similar to that of the 559 nm feature (e.g., that of one low-spin ferric heme) and therefore 2−3 times too large to arise from typical high-spin heme. Therefore, it appears that the α-band of one of the low-spin ferric hemes (probably heme *b*) is relatively blue-shifted compared to that of the *Ps. stutzeri* enzyme, appearing near 600 nm and overlapping with the CT ("630") band arising from high-spin heme b_3. We do not yet know the significance of these differences between NORs obtained from these two bacteria. However, the result of the blue shift of one of the bands in the MCD spectrum of the *P. denitrificans* enzyme is that the weak CT ("630") band is not resolved, but may contribute to the broad negative lobe of the 595 nm derivative.

In the near-infrared (NIR) MCD spectrum (Figure 1C), two CT bands typical of low-spin ferric hemes are observed at ~1560 and ~1800 nm. These are comparable to those reported for the *Ps. stutzeri* enzyme (*6*) and confirm the presence of bis-histidine and histidine and/or methionine axial ligation states for hemes *b* and *c*, respectively.

These MCD assignments are consistent with the low-temperature X-band perpendicular-mode EPR spectrum of the same sample (Figure 2), which shows the presence of two low-spin ferric hemes in approximately equal concentrations. One gives a typical *rhombic* spectrum (g_z, g_y, and g_x = 3.00, 2.25, and 1.46) virtually identical to those observed for the magnetically isolated ferric heme in subunit I of many heme−copper oxidases, including bovine C*c*O (*18*), *Escherichia coli* cytochrome bo_3 (*19*), and cytochrome cbb_3 from *Rhodobacter capsulatus* (*20*). Given the conservation of secondary structure in this class of proteins, it is reasonable to assume that these signals comprise the spectrum of a low-spin ferric heme *b* in NorB, with the highly conserved histidine residues in helices II (His-53) and X (His-336) acting as axial ligands. The other is a high-g_{max} species for which only the $g_z = 3.55$ feature is observed. This we assign to low-spin ferric heme *c* in NorC for which the conserved residues His-65 and Met-115 serve as axial ligands. Examples of histidine and/or methionine coordination leading to high-g_{max} spectra are well described (*21*, *22*).

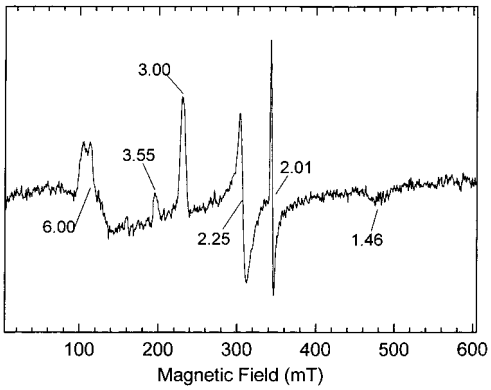

FIGURE 2: X-Band EPR spectrum of oxidized *P. denitrificans* NOR. The spectrum was recorded at 10 K using the following conditions: a microwave frequency of 9.44 GHz and a microwave power of 2 mW. Signals near $g = 6$ arise from substoichiometric (<5%) amounts of high-spin heme, while the sharp derivative at $g = 2.01$ is due to a trace of a contaminating [3Fe-4S] cluster. There are no signals arising from the magnetically coupled dinuclear center.

Mediated Redox Titrations. The midpoint redox potentials of the Fe(II)/Fe(III) couples were measured via their absorption spectra in the visible region (500−700 nm) at a number of known redox potentials (E_h) in the range of −100 to 400 mV. As E_h was lowered from 400 to 145 mV, the low-spin *c* and *b* hemes both became reduced, as judged from the increase in the absorption of the α-bands at 551 nm (heme *c*, Figure 3A) and 560 nm (heme *b*, Figure 3B). The absorption increases at each of these wavelengths were plotted as a function of E_h, and both data sets could be described by single $n = 1$ Nernstian components. From these simulations, midpoint redox potentials of 310 and 345 mV were calculated for the Fe(II)/Fe(III) couples of heme *c* (Figure 3A) and heme *b* (Figure 3B), respectively. These values are on the same order of magnitude as those reported for the same centers in NOR from *Ps. stutzeri* (*23*). The intensity of the CT ("630") band monitored at 595 nm decreased as E_h was lowered (Figure 3C). This decrease in intensity is described by two sequential $n = 1$ Nernstian components yielding midpoint redox potentials of 320 and 60 mV, respectively (Figure 3C). Examination of spectra collected at defined potentials revealed that the first phase is caused by an apparent shift of the CT band to 604 nm and that the second phase is due to the disappearance of this red-shifted band (Figure 4A). The persistence of a CT band after the first phase of reduction suggests that only Fe_B(III)

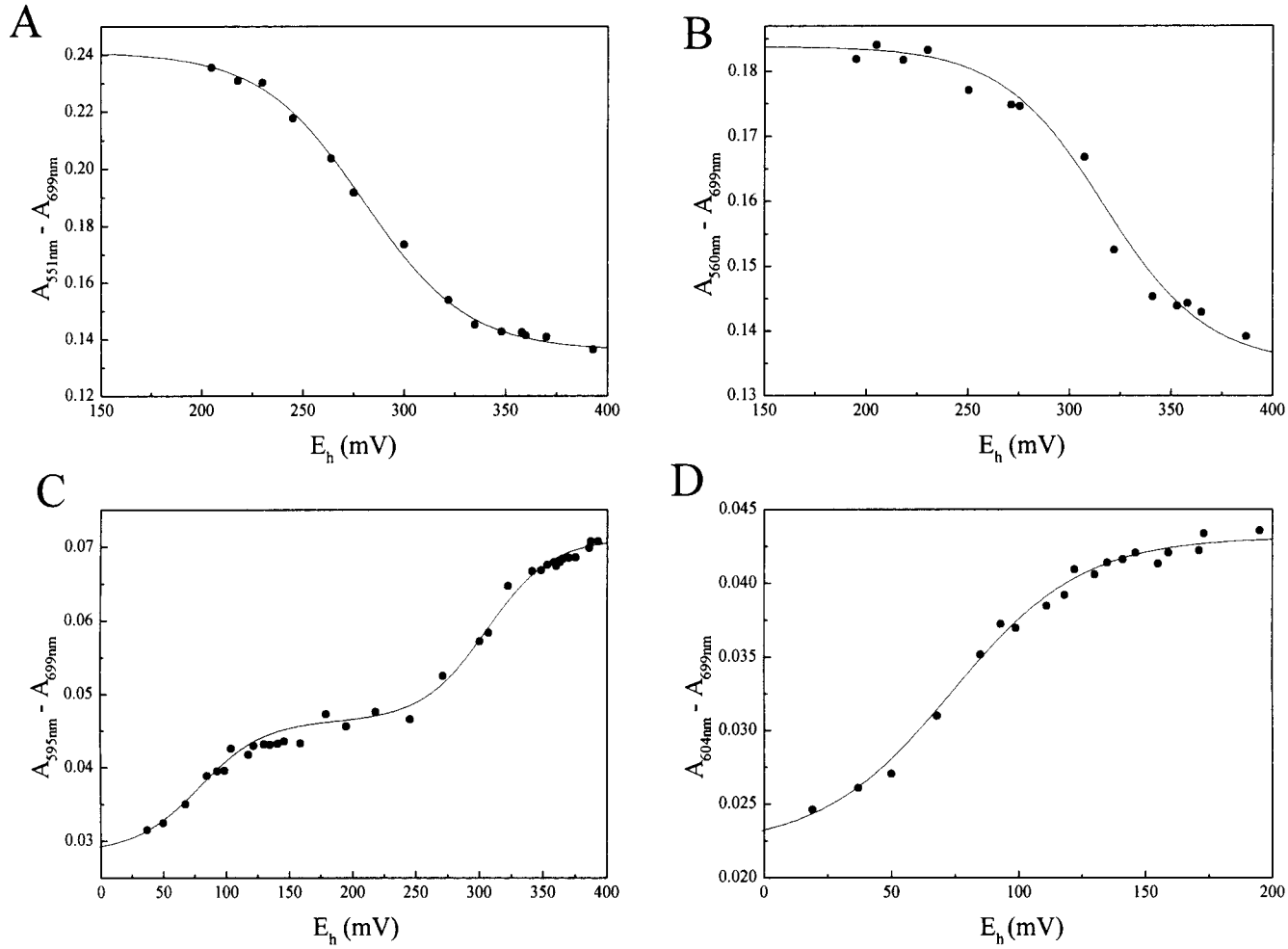

FIGURE 3: Mediated redox titrations of the metal centers in *P. denitrificans* NOR: (A) heme *c* (551 nm minus 699 nm), (B) heme *b* (560 nm minus 699 nm), (C) heme b_3 (595 minus 699 nm), and (D) heme b_3 (604 minus 699 nm). Reductive titrations were carried out as described in Materials and Methods. Duplicate experiments in which the enzyme was fully reduced and titrated with oxidant gave identical results (not shown). In panels A, B, and D, the data are fitted to single $n = 1$ Nernstian components with E_m values of 310 and 345 mV. In panel C, the data are fitted to two $n = 1$ Nernstian components with an E_m of 320 mV (66%) and an E_m of 60 mV (34%).

is reduced while heme b_3 remains oxidized. Therefore, the bleaching of the 604 nm CT band ($E_m = 60$ mV; Figure 3D) must be due to reduction of heme b_3.

Spectroscopic Characterization of the Three-Electron-Reduced NOR. The large separation of the midpoint redox potentials of Fe_B ($E_m = 320$ mV) and heme b_3 ($E_m = 60$ mV) is >200 mV which allows NOR to be poised in a three-electron-reduced state. NOR was poised at 150 mV in the presence of appropriate mediators (see Materials and Methods) both chemically (with dithionite) and in a potentiostat. The electronic absorption spectrum of the sample poised chemically has intense α,β bands that are associated with fully reduced *b*- and *c*-type hemes. In addition, the CT ("630") band remains, indicating that heme b_3 is fully oxidized (Figure 4A). The apparent decrease in intensity of the CT band upon reduction of Fe_B occurs because in the oxidized enzyme the CT band centered at 595 nm is superimposed on a transition arising from low-spin ferric heme *b*. This intensity is lost upon reduction, and the center of the CT band moves to lower energy so that the two bands no longer overlap.

Figure 4B shows the room-temperature MCD spectrum of three-electron-reduced NOR. A narrow derivative feature near 550 nm, with structure to higher energy, is the characteristic fingerprint of low-spin ferrous heme. The spectrum near 550 nm arises from two overlapping sharp derivative bands which are assigned to reduced hemes *b* and *c*. The Soret intensity is also due largely to these two ferrous hemes. In addition, the loss of the very weak derivative-shaped feature around 700 nm can also be attributed to reduction of heme *c*. There are no bands characteristic of *high-spin* ferrous heme which would also give rise to a derivative-shaped Soret band but with the opposite sign compared to that of its low-spin counterpart and with a higher intensity. The features observed in the 580−640 nm region are two weak ($\sim$10 M^{-1} cm^{-1} T^{-1}) overlapping derivatives which we assign as the high-spin ferric CT bands arising from heme b_3 in the dinuclear center.

DISCUSSION

We have determined the midpoint redox potentials of each of the metal centers in the two-subunit form of NOR from *P. denitrificans*. Three of the centers (heme *c*, heme *b*, and Fe_B) have approximately the same potential in the range of 300−350 mV. This would allow rapid transfer of electrons from the presumed physiological electron donors, pseudoazurin ($E_m = 230$ mV) (*24*) and cytochrome c_{550} ($E_m = 256$ mV) (*25*), to Fe_B in the active site. The rather low potential

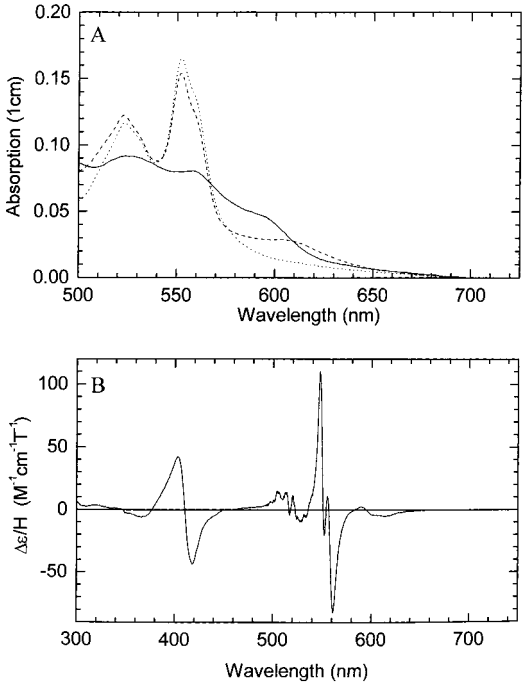

FIGURE 4: Effect of redox potential on the electronic absorption and RT-MCD spectra of *P. denitrificans* NOR. (A) Visible region electronic absorption spectra collected at E_h values of 440 (—), 145 (– – –), and 4 mV (–•–•–) during the mediated redox titrations whose results are shown in Figure 3. (B) RT-MCD spectrum of *P. denitrificans* NOR (35 μM) poised at an E_h of 150 mV in a potentiostat as described in Materials and Methods.

of heme b_3 ($E_m = 60$ mV), some 200 mV below the midpoint redox potentials of heme *b* and Fe_B, represents a considerable thermodynamic barrier to the complete (two-electron) reduction of the dinuclear center.

Since there are unique spectral features associated with each of the three hemes, measurement of the midpoint potentials of the redox centers of NOR by mediated redox potentiometry is straightforward. In C*c*O, the midpoint redox potential of heme *a* is difficult to determine due to the spectral overlap of hemes *a* and a_3, and from the apparent interaction of heme *a* with the other redox centers in the protein (*26*−*28*). There is no reason to propose such redox interactions between the metal centers of NOR to simulate the redox titrations shown in Figure 3. This is perhaps not surprising as it has been suggested that the negative redox cooperativity exhibited by the hemes in C*c*O is necessary for avoiding short-circuiting the proton pump (*29*). Since NOR is not electrogenic (*16*), there is perhaps not the same requirement for such interactions between the redox centers.

Given the close structural relationship between NorB and subunit I of the heme−copper oxidases, it is interesting to consider the relative values of the midpoint redox potentials of the two hemes in each class of enzymes. Despite the difficulties of measurement, there is a reasonable consensus as to the value of the midpoint redox potential of heme *a* in the bovine C*c*O which is usually quoted as being on the order of 330 mV (*27*, *28*). Similar values have been reported for the midpoint redox potentials of heme *a* in the C*c*Os purified from yeast (*30*) and *Rhodobacter sphaeroides* (*31*).

The values obtained for the midpoint redox potential of heme a_3 in mediated redox titrations are influenced not only by interactions with other redox centers in the protein but also by the well-known heterogeneity exhibited by the dinuclear centers of heme−copper oxidases (see ref *32* and references therein). Therefore, it may be better to consider the separation of the midpoint redox potentials of hemes *a* and a_3. This can be derived by measuring the intrinsic rate of electron transfer between the two hemes in both bovine C*c*O and bacterial heme−copper oxidases (*33*, *34*). The observed rate constant together with the inter-heme distance suggests a driving force ($\Delta G°$) of between 0 and −4 kJ mol^{-1} that would correspond to a separation of the midpoint redox potentials in the range of 0−50 mV, considerably lower than the 200 mV difference we observe for NOR.

If reduction of heme b_3 in NOR is not favored, we must consider if this has any implications for the possible role(s) of the dinuclear center in catalyzing the two-electron reduction of NO to N_2O. This should also take into account the rather different role of the dinuclear center in the heme−copper oxidases that have evolved to catalyze the four-electron reduction of O_2 to H_2O. The free energy released from this reaction is used to pump four protons that contribute to a transmembrane proton gradient. The first half-reaction in this catalytic cycle involves the kinetic trapping of oxygen as peroxide at the dinuclear center heme (*29*). This requires the weak binding of dioxygen to ferrous heme at the two-electron-reduced dinuclear center, followed by the rapid transfer of electrons from both hemes to the bound oxygen (*35*).

The mechanism by which NOR catalyzes the two-electron reduction of NO to N_2O has not yet been resolved. It has been suggested that single equivalents of NO bind to both $Fe(II)_B$ and Fe(II) heme b_3 (*12*). EPR signals that can be assigned to both $Fe(II)_B$−NO and Fe(II)−heme b_3−NO have been reported in turnover (*11*). This arrangement would orientate the two NO molecules to favor N−N bond formation. (*6*, *12*). The subsequent elimination of N_2O from the Fe(II)−NO::ON−Fe(II) ligated dinuclear center (*12*) would yield either a μ-oxo or hydroxyl species bridging heme b_3 and Fe_B. Such a bridge may mediate magnetic coupling between the two centers, which is one possible explanation for the absence of signals arising from Fe(III)−heme b_3 or $Fe(III)_B$ in the EPR spectrum of oxidized NOR (Figure 2).

When such a mechanism is considered, it should be remembered that the dissociation constant for the Fe(II)−heme *b*−NO complex in myoglobin is reported to be 7×10^{-12} M (*36*). Such tight binding of NO to Fe(II)−heme b_3 would not be compatible with turnover of the enzyme. Therefore, we presume either that the environment of the dinuclear center of NOR weakens the binding of NO to Fe(II)−heme b_3 or that heme b_3 has an alternative role in NO reduction. In this context, it is worth noting that cytochrome bo_3 from *E. coli* can bind 2 equiv of NO to $Cu(II)_B$ (*37*). This unexpected observation led to the proposal that NO reduction in heme−copper oxidases takes place exclusively at Cu_B (*38*). A modified version of this mechanism can describe catalysis in bacterial NOR. In this proposed scheme, the low midpoint redox potential of heme b_3 would ensure that this center remained oxidized and that formation of ferrous−nitrosyl heme did not occur.

The obvious spectral feature associated with ferric heme b_3 in oxidized NOR (the shoulder at 595 nm), combined with the low midpoint redox potential of heme b_3, makes it possible to explore the consequences of introducing a single

electron into the dinuclear center of NOR. By analogy to the structure of C*c*O, it is likely that the dinuclear center of NOR lies in an environment with a low dielectric constant, and that the energetic cost of introducing negative charge at this site is high (*39*). In the case of C*c*O, the introduction of a negative charge into the heme−copper dinuclear center, either by reduction or by binding an anion at that site, must be strictly balanced by the uptake of a proton (*40*). It is tempting to presume that the apparent shift in the position of the CT band on reduction of Fe_B represents protonation of the axial hydroxide ligand. However, even at 604 nm, the CT ("630") band would be considerably more blue-shifted than any other example we have seen of histidine and/or H_2O ligated high-spin Fe(III)−heme (*38*, *41*). Therefore, we believe that after reduction of Fe_B, the sixth ligand of heme b_3 continues to be a hydroxide ion, and that the spectral changes we observe report a proton binding elsewhere in the dinuclear center, possibly to a nearby amino acid side chain.

This may be of interest because primary sequence analysis shows that the region of helix VI close to the NOR dinuclear center is very different from the same region in subunit I of C*c*Os, although these amino acid sequences are highly conserved within each class of enzymes (*1*). NOR does not contain a residue equivalent to the conserved glutamate at position 278 of *P. denitrificans* C*c*O subunit I. This residue which lies at the head of the so-called D channel is highly conserved and required to move protons required for both the reduction of bound peroxide to water and establishing a transmembrane proton gradient. Instead, helix VI of NorB contains two conserved glutamates (at positions 198 and 202 of the *P. denitrificans* NorB sequence) that are conserved in all nine[3] known NorB sequences (*1*), but not in subunit I of heme−copper oxidases (*1*). The glutamate at position 198 lies one helical turn below the putative Fe_B ligand His-194. Substitution of Glu-198 with an alanine residue abolishes catalytic activity (G. Butland, unpublished data). In contrast, changing Glu-202 to an alanine has little or no effect on catalysis. We have previously noted that non-heme iron prefers an octahedral coordination environment rather than the distorted tetrahedral environment favored by Cu_B (*1*, *42*). Consequently, NOR may employ Glu-198 as an additional ligand to Fe_B. However, there are other candidates for this role, notably, the conserved glutamate at position 267 in helix VIII (*42*). If Glu-267 were to function as an additional ligand to FeB, then the proximity of Glu-198 to the dinuclear center would make it an excellent candidate for serving as a base during reduction of the active site.

Both NOR and heme−copper oxidases evolved from a common ancestor (*43*). It is possible that the ancestral oxidase utilized iron rather than copper in the dinuclear center because, under the highly reducing conditions of the primordial biosphere, ferrous ions were more readily available than insoluble cuprous ions. It is thought to be likely that denitrification evolved before aerobic respiration in the biosphere and that the primary function of the ancestral oxidase was the reduction of NO (*43*). Hence, it has been argued that a key step in the evolution of aerobic life on earth was the substitution of iron by copper in the ancestral oxidase, allowing it to efficiently reduce oxygen (*1*, *3*, *4*, *42*). However, the data presented here suggest that a change in the elemental composition of the dinuclear center may itself not be enough to endow high oxidase activity. Clearly, energy-conserving heme−copper oxidases needed to gain two other features. First, they needed to change the environment around the catalytic site that raised the midpoint redox potential of the dinuclear center heme sufficiently to favor both oxygen binding and rapid heme−heme electron transfer. Second, they needed to evolve proton channels that allowed movement of both substrate and pumped protons from the cytoplasm to the active site.

[3] Thus far, nine *norB* type genes have been sequenced. These are from *P. denitrificans*, *Paracoccus halodenitrificans*, *Ps. stutzeri*, *Pseudomonas aeruginosa*, *R. sphaeroides*, *Ralstonia eutropha* (two isozymes), *Synnochocystis* strain PCC 6803, and *Mycobacterium avium*. Five organisms, *P. denitrificans*, *P. halodenitrificans*, *Ps. stutzeri*, *Ps. aeruginosa*, and *R. sphaeroides*, contain a *norC* gene in the same cluster as *norB*. The rest appear to have no NorC homologue, but instead have a 200-amino acid N-terminal extension to NorB that lacks a cytochrome *c* binding motif. Whatever the source of NorB, the glutamates in transmembrane helices IV (E125), VI (E198 and E202), and VII (E267) are absolutely conserved. A limited alignment comparing transmembrane helices VI−VIII to the equivalent regions in the heme−copper oxidases can be found in ref *1*.

ACKNOWLEDGMENT

We thank Dr. Rob Van Spanning (Vrije Univesiteit, Amsterdam, The Netherlands) for his generous gift of *P. denitrificans* 93.11. This work was considerably facilitated by the excellent technical contributions of both Carol Robinson and Jeremy Thornton.

REFERENCES

1. Watmough, N. J., Butland, G., Cheesman, M. R., Moir, J. W. B., Richardson, D. J., and Spiro, S. (1999) *Biochim. Biophys. Acta 1411*, 456−474.
2. Richardson, D. J., and Watmough, N. J. (1999) *Curr. Opin. Chem. Biol. 3*, 207−219.
3. Hendriks, J., Gohlke, U., and Saraste, M. (1998) *J. Bioenerg. Biomembr. 30*, 15−24.
4. Saraste, M., and Castresana, J. (1994) *FEBS Lett. 341*, 1−4.
5. van der Oost, J., deBoer, A. P. N., deGier, J.-W. L., Zumft, W. G., Stouthamer, A. H., and van Spanning, R. J. M. (1994) *FEMS Microbiol. Lett. 121*, 109.
6. Cheesman, M. R., Zumft, W. G., and Thomson, A. J. (1998) *Biochemistry 37*, 3994−4000.
7. Iwata, S., Ostermeier, C., Ludwig, B., and Michel, H. (1995) *Nature 376*, 660−669.
8. Tsukihara, T., Aoyama, H., Yamashita, E., Tomizaki, T., Yamaguchi, H., Shinzawa-Itoh, K., Nakashima, R., Yaono, R., and Yoshikawa, S. (1995) *Science 269*, 1069−1074.
9. Oganesyan, V., Cheesman, M. R., Butler, C., Watmough, N., Greenwood, C., and Thomson, A. (1998) *J. Am. Chem. Soc. 120*, 4232−4233.
10. Heiss, B., Frunzke, K., and Zumft, W. G. (1989) *J. Bacteriol. 171*, 3288−3297.
11. Hendriks, J., Warne, A., Gohlke, U., Haltia, T., Ludovici, C., Lubben, M., and Saraste, M. (1998) *Biochemistry 37*, 13102−13109.
12. Girsch, P., and de Vries, S. (1997) *Biochim. Biophys. Acta 1318*, 202−216.
13. Carr, G. J., and Ferguson, S. J. (1990) *Biochem. J. 269*, 423−429.
14. de Boer, A. P., van der Oost, J., Reijnders, W. N., Westerhoff, H. V., Stouthamer, A. H., and van Spanning, R. J. (1996) *Eur. J. Biochem. 242*, 592−600.
15. de Gier, J.-W. L., Lübben, M., Reijnders, W. N. M., Tipker, C. A., van Spanning, R. J. M., Stouthamer, A. H., and van der Oost, J. (1994) *Mol. Microbiol. 13*, 183−196.

16. Bell, L. C., Richardson, D. J., and Ferguson, S. J. (1992) *J. Gen. Microbiol. 138*, 437−443.
17. Dutton, P. L. (1978) *Methods Enzymol. 54*, 411−435.
18. Aasa, R., Albracht, S. P. J., Falk, K.-E., Lanne, B., and Vanngård, T. (1976) *Biochim. Biophys. Acta 422*, 260−272.
19. Cheesman, M. R., Watmough, N. J., Pires, C. A., Turner, R., Brittain, T., Gennis, R. B., Greenwood, C., and Thomson, A. J. (1993) *Biochem. J. 289*, 709−718.
20. Gray, K. A., Grooms, M., Myllykallio, H., Moomaw, C., Slaughter, C., and Daldal, F. (1994) *Biochemistry 33*, 3120−3127.
21. Gadsby, P. M., Hartshorn, R. T., Moura, J. J., Sinclair-Day, J. D., Sykes, A. G., and Thomson, A. J. (1989) *Biochim. Biophys. Acta 994*, 37−46.
22. Spinner, F., Cheesman, M. R., Thomson, A. J., Kaysser, T., Gennis, R. B., Peng, Q., and Peterson, J. (1995) *Biochem. J. 308*, 641−644.
23. Kastrau, D. H. W., Heiss, B., Kroneck, P. M. H., and Zumft, W. G. (1994) *Eur. J. Biochem. 222*, 293−303.
24. Martinkus, K., Kennelly, P. J., Rea, T., and Timkovich, R. (1980) *Arch. Biochem. Biophys. 199*, 465−472.
25. Samyn, B., Berks, B. C., Page, M. D., Ferguson, S. J., and Van Beeumen, J. J. (1994) *Eur. J. Biochem. 219*, 585−594.
26. Blair, D. F., Ellis, W. R., Jr., Wang, H., Gray, H. B., and Chan, S. I. (1986) *J. Biol. Chem. 261*, 11524−11537.
27. Kojima, N., and Palmer, G. (1983) *J. Biol. Chem. 258*, 14908−14913.
28. Mitchell, R., Mitchell, P., and Rich, P. R. (1991) *FEBS Lett. 280*, 321−324.
29. Babcock, G. T., and Wikström, M. (1992) *Nature 356*, 301−309.
30. Meunier, B., Ortwein, C., Brandt, U., and Rich, P. R. (1998) *Biochem. J. 330*, 1197−1200.
31. Jünemann, S., Meunier, B., Gennis, R. B., and Rich, P. R. (1997) *Biochemistry 36*, 14456−144564.
32. Moody, A. J. (1996) *Biochim. Biophys. Acta 1276*, 6−20.
33. Ädelroth, P., Brzezinski, P., and Malmström, B. G. (1995) *Biochemistry 34*, 2844−2849.
34. Morgan, J. E., Verkhovsky, M. I., Puustinen, A., and Wikström, M. (1993) *Biochemistry 32*, 11413−11418.
35. Verkhovsky, M. I., Morgan, J. E., Puustinen, A., and Wikström, M. (1996) *Nature 380*, 268−270.
36. Brucker, E. A., Olson, J. S., Ikeda-Saito, M., and Phillips, G. N. J. (1998) *Proteins 30*, 352−356.
37. Butler, C. S., Seward, H. E., Greenwood, C., and Thomson, A. J. (1997) *Biochemistry 36*, 16259−16266.
38. Watmough, N. J., Cheesman, M. R., Butler, C. S., Little, R. H., Greenwood, C., and Thomson, A. J. (1998) *J. Bioenerg. Biomembr. 30*, 55−62.
39. Rich, P. R. (1995) *Aust. J. Plant Physiol. 22*, 479−486.
40. Mitchell, R., and Rich, P. R. (1994) *Biochim. Biophys. Acta 1186*, 19−26.
41. Cheesman, M. R., Watmough, N. J., Gennis, R. B., Greenwood, C., and Thomson, A. J. (1994) *Eur. J. Biochem. 219*, 595−602.
42. Berks, B. C., Ferguson, S. J., Moir, J. W., and Richardson, D. J. (1995) *Biochim. Biophys. Acta 1232*, 97−173.
43. Castresana, J., and Saraste, M. (1995) *Trends Biochem. Sci. 20*, 443−448.

BI9916426